

Ordered monolayer structures of boron in Si(111) and Si(100)

R. L. Headrick

Cornell High Energy Synchrotron Source and Department of Applied and Engineering Physics, Cornell University, Ithaca, New York 14853

B. E. Weir, A. F. J. Levi, B. Freer, J. Bevk, and L. C. Feldman

AT&T Bell Laboratories, Murray Hill, New Jersey 07974

(Received 31 January 1991; accepted 16 February 1991)

We have prepared metastable, ordered monolayer structures of boron on Si(100) and Si(111) by silicon deposition atop unique surface reconstructions. These superlattice structures suggest possibilities for monolayer doping and ordered alloy structures with new electronic properties. In this paper we summarize our recent results in forming ordered structures and the electrical properties of the preserved layers.

I. INTRODUCTION

Ordered surface reconstructions are not only stable at the solid-vacuum interface, but can be preserved as metastable structures at solid-solid interfaces. In the *a*-Si/Si(111) system, the complex 7×7 structure can be preserved at the interface formed by the clean Si(111)- 7×7 surface and subsequent deposition of amorphous silicon (*a*-Si).¹ More recently, it was shown that the $\sqrt{3} \times \sqrt{3}$ boron structure can be partly preserved under epitaxial silicon.²⁻⁴ In this paper we review our recent observations of buried structures in systems consisting of ordered boron adsorbates on $\langle 111 \rangle$ and $\langle 100 \rangle$ oriented Si surfaces.³⁻⁶ These atomic configurations behave electrically as a dopant sheet of atoms with high electrical activity.⁵⁻⁷ In the $\langle 100 \rangle$ case, a highly ordered *p*-type monolayer with 100% electrical activity is prepared within defect-free crystalline silicon.⁷ As part of these studies, the minimum epitaxial growth temperature for 100–350-Å films of silicon on $\langle 100 \rangle$ and $\langle 111 \rangle$ surfaces was determined, and it was found that $\langle 100 \rangle$ growth occurs 300 K lower than $\langle 100 \rangle$ growth.⁸

II. EXPERIMENTAL

Samples were prepared in a molecular-beam epitaxy chamber equipped with an electron gun evaporator to deposit silicon, a quartz-crystal thickness monitor, and a Knudsen cell to deposit boron from HBO₂. Oriented $\langle 111 \rangle$ and $\langle 100 \rangle$ Si substrates were prepared by chemical growth of a thin protective oxide layer, and then transferred into the vacuum chamber. Once in the vacuum chamber, the oxide was desorbed from the sample and boron was deposited onto the surface up to a coverage of between zero and one monolayer. After cooling to room temperature, low-energy electron diffraction (LEED) and Auger electron spectroscopy (AES) measurements were performed. Finally, the surface was capped with silicon at various temperatures. All other measurements, including grazing incidence x-ray diffraction (XRD), ion scattering/channeling, transmission electron microscopy, and low-temperature ($T = 4.2$ K) Hall effect measurements were done after removing the capped samples from the vacuum system. In a separate set of experiments, silicon layers of 100–300-Å thickness were grown on $\langle 100 \rangle$ and $\langle 111 \rangle$ oriented silicon at various temperatures. An ion channeling analysis using 1.8-MeV ⁴He⁺ was used to deter-

mine the epitaxial quality as a function of growth temperature.

III. Si(111)-B SURFACE RECONSTRUCTION

Glancing angle x-ray diffraction and first-principles theoretical calculations have established the structure of the Si(111)-B $\sqrt{3} \times \sqrt{3}$ reconstruction as subsurface substitutional boron arranged in a $\sqrt{3} \times \sqrt{3}$ configuration.^{4,9} Figure 1 shows this site and compares it to the more common $\sqrt{3} \times \sqrt{3}$ configuration (*T*₄ site) for Ga and other adsorbates. The nominal B(Ga) coverage is 1/3 monolayer; one of every three sites in a single atomic layer is occupied by B(Ga). The stability of boron in the subsurface site relative to the *T*₄ adatom site is related to relief of subsurface strain by the mechanism of substituting a smaller boron atom for silicon.⁴

The fact that this ordered structure is maintained upon room-temperature deposition of *a*-Si is shown in Fig. 2, which compares the glancing angle x-ray diffraction of both the Ga and B structures. Both samples were capped with 50 Å of *a*-Si and rocking scans through the $(2/3, 2/3)$ superlattice reflection were performed at $q_1 = 0.2(2\pi/d_{111})$, where

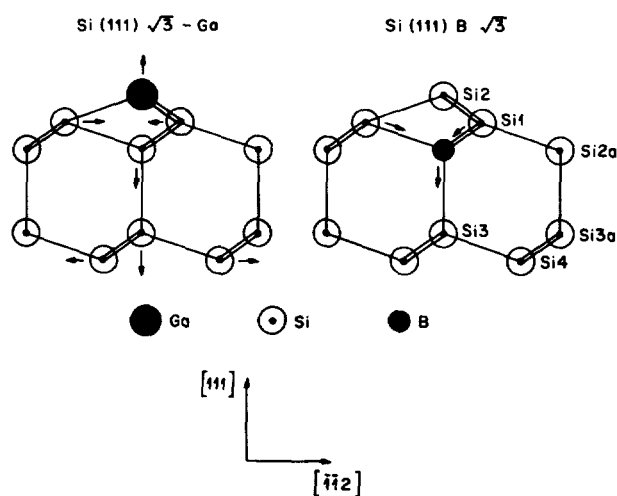


FIG. 1. Model of the Si(111)- $\sqrt{3}$ Ga structure and proposed structure for Si(111):B $\sqrt{3}$ (right). Arrows indicate the direction of displacements from the ideal tetrahedrally bonded configuration.

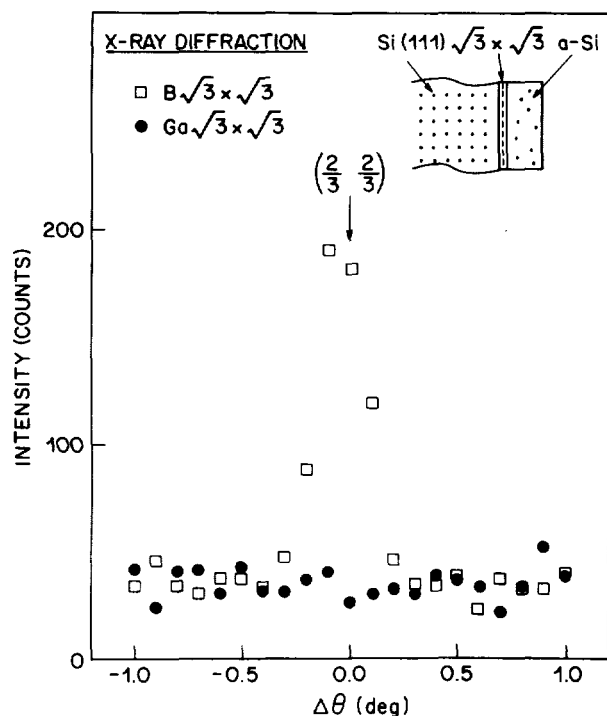


FIG. 2. Rocking scan through the $(2/3, 2/3)$ surface x-ray diffraction rod for buried boron and gallium surface structures on Si(111). The intensity units refer to reflectivity in counts per constant integrated incident beam flux.

$d_{111} = 3.135 \text{ \AA}$. Retention of the strong one-third order diffraction intensity in the boron case clearly indicates that the boron retains its $\sqrt{3} \times \sqrt{3}$ structure while Ga becomes disordered. Detailed Auger measurements show that the Ga surface segregates during Si deposition at room temperature, while boron remains in a buried, ordered configuration. Surface segregation of dopant or impurity atoms during epitaxial growth is commonly observed although it may be kinetically limited at low growth temperatures. The difference in surface segregation between B and Ga suggests that the surface site influences the segregation behavior. Such segregation behavior is consistent with the buried site for boron and an atop site for Ga.

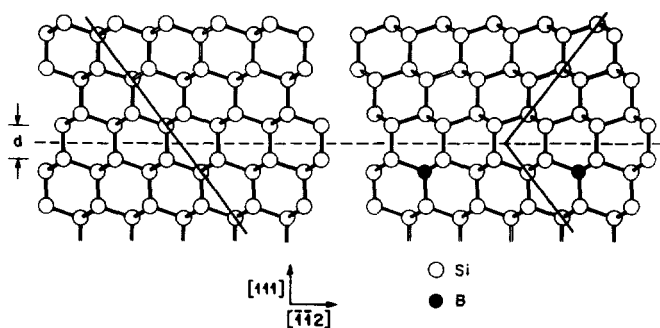


FIG. 3. Ball and stick models for the film orientation and interface structure for 0- (left) and 0.33-ML (right) boron coverages. The $\sqrt{3} \times \sqrt{3}$ reconstruction of the interface is introduced because boron occupies substitutional sites, occupying every third site in a single monolayer at the interface.

IV. GROWTH ON SI(111)-B

The adatom structure of the boron $\sqrt{3} \times \sqrt{3}$ surface is a "chemically passivated" surface in that it contains no dangling bonds.⁹ Therefore, it is somewhat surprising that epitaxial silicon can grow on this surface. We have recently shown that the silicon adatoms terminating the surface are efficiently displaced from ordered sites by deposited silicon, thus allowing epitaxial silicon to grow in a continuation of the bulk crystal structure.⁴ However, an interesting phenomenon is observed for Si epitaxial growth on this surface: Evidently the initial layers of silicon are strongly influenced by the interaction with the boron monolayer, giving rise to a 180° rotated configuration of the grown layer of Si (Fig. 3). The existence of this layer is most strikingly demonstrated in Fig. 4, which shows a comparison of $(1,0,l)$ crystal truncation rod data to structure factors calculated in the kinematic approximation for a 350-Å silicon film grown at 400 °C and annealed at 1000 °C for 2 h (Fig. 4). The dashed line is the square of the structure factor $F_{10}(l)$ for the semi-infinite silicon substrate with double-layer termination. There are three prominent peaks that do not correspond to the substrate that can be accounted for by adding the 350-Å-thick rotated film into the calculated structure factor. The solid line shows the results of calculations with a 233 monolayer, rotated layer, with an optimum interface separation of $d = 2.35 \pm 0.09 \text{ \AA}$, i.e., the same as the bulk layer spacing. Transmission electron microscopy confirms this assignment showing that the layer is at least 90% crystallographically pure.¹⁰

Recent experiments have shown that high-temperature ($\sim 550 \text{ }^\circ\text{C}$) deposition of Si results in boron disordering and

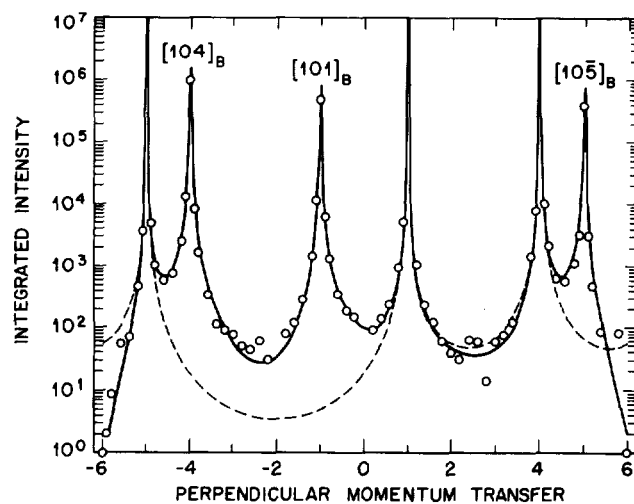


FIG. 4. $(1,0)$ rodscan for a 350-Å rotated Si film on Si(111). A four-circle diffractometer and Cu $K\alpha$ radiation was used for the measurement. The diffraction profiles are indexed relative to a hexagonal unit cell appropriate for the Si(111) surface with in-plane lattice parameters $a = b = 3.84 \text{ \AA}$ and out-of-plane lattice parameter $c = 9.41 \text{ \AA}$. The hexagonal indices are derived from cubic indices by $[10l]_{\text{hex}} \equiv 1/3[422]_{\text{cub}} + l/3[111]_{\text{cub}}$. Rotated reflections are indexed by replacing l by $-l$. Structure factors at $-l$ were obtained by the symmetry relation $[01l]$. The dashed line is the calculated intensity from a "bulk-like" structure, the full line is for a 350-Å rotated film atop a bulk crystal.

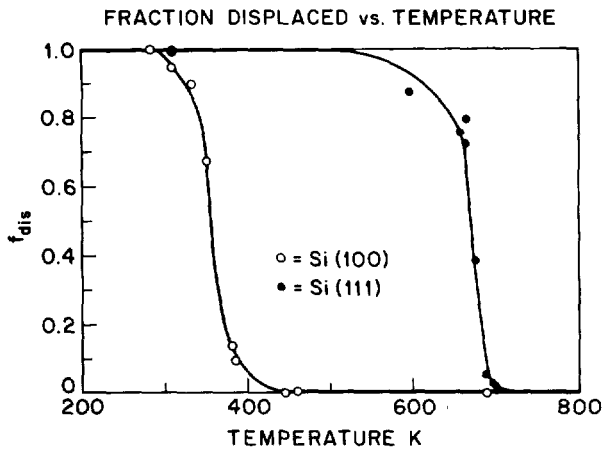


FIG. 5. Ion channeling yield vs growth temperature of thin silicon films on Si(100) and Si(111).

surface segregation, indicating that the metastable structure associated with the ordered δ layer is not stable at Si epitaxy temperatures.³ Even at the lowest temperature for Si(111) epitaxy ($\sim 400^\circ\text{C}$), some boron disordering occurs and the epitaxial film remains defective. Therefore, preservation of the $\sqrt{3}\times\sqrt{3}$ structure within a defect-free crystalline silicon has not, so far, been possible. This has prompted a systematic investigation of low-temperature epitaxial growth which we discuss below.

V. TEMPERATURE DEPENDENCE OF SILICON MOLECULAR-BEAM EPITAXY

In order to determine the minimum temperature required to grow 100–350-Å films, channeling measurements were carried out with 1.8-MeV $^4\text{He}^+$ using a grazing exit angle geometry.⁸ Channeled ions are scattered by atoms displaced from bulk crystal sites, e.g., those in amorphous material or those in material misoriented during growth. Figure 5 shows the temperature dependence of the fraction of disordered atoms for 300-Å films grown on (111) oriented silicon, with a sharp decrease near 400 °C, the transition to higher crystal quality. Also shown in Fig. 5 is data for 300-Å films, grown on Si(100) at the same rate of 0.3 Å/s. A remarkable difference in transition temperature is to be noted. The Si(100) transition is in reasonable agreement with the recently published results of Eaglesham et al.,¹¹ which yield a 160 °C transition temperature for 300-Å film grown at 0.7 Å/s.

The difference in the temperatures needed for epitaxial growth on Si(100) and Si(111) is thought to be related to the difference in bonding geometry on the two surfaces. Silicon atoms deposited onto (111) surfaces tend to occupy "adatom" or "faulted" sites that are not a continuation of the bulk crystal structure. In contrast, silicon atoms deposited onto (100) surfaces have the possibility of relaxing directly into bulk-like epitaxial sites. Molecular-dynamics simulations also predict a much higher growth temperature on (111) oriented surfaces, and confirm these ideas.⁸ Growth on (100) oriented silicon is thus greatly preferred for preserving ordered structures and suppressing surface segregation.

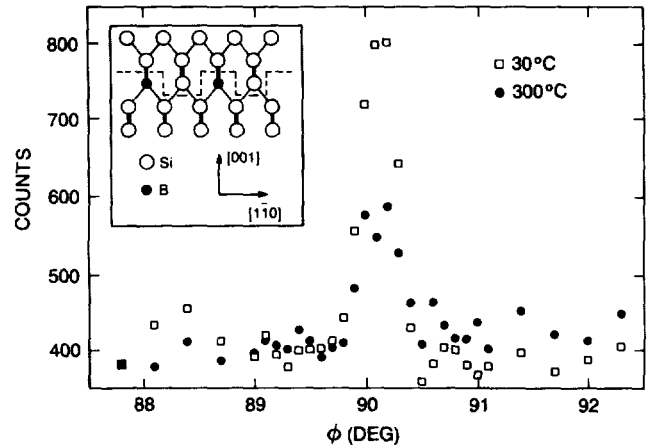


FIG. 6. Comparison of grazing incidence x-ray diffraction azimuthal scans through the (3/2,0) diffraction spot for Si(100)-(2 \times 1) boron buried structures capped by growth at room temperature, and at $\approx 300^\circ\text{C}$. The boron coverage was 1/2 monolayer in both cases and the silicon growth rate was 0.1 Å/s. The inset shows a proposed model of the (2 \times 1) structure.

VI. GROWTH ON Si(100)-B

We have recently reported a boron-induced (2 \times 1) surface reconstruction at 1/2 monolayer boron coverage on (100) oriented silicon.⁷ In sharp contrast to the results on (111) oriented silicon discussed above, we find that this reconstruction can be preserved within high quality, *crystalline* silicon by low-temperature epitaxial overgrowth at $\approx 300^\circ\text{C}$. For boron coverages at and below the completion of the (2 \times 1) surface phase and silicon overlayer growth temperatures of 300 °C and above, 100% of the boron is electrically active.

Figure 6 shows grazing incidence x-ray diffraction azimuthal scans through (3/2,0) surface reflections for two ordered interfaces. The open squares are for a 100-Å silicon overlayer grown at room temperature, and the filled circles are for a 100-Å silicon overlayer grown at 300 °C. The boron coverage is 1/2 monolayer in both cases. The reconstruction with overgrowth at 300 °C gives a factor of 2 smaller integrated intensity in the diffraction signal than the reconstruction after growth at room temperature. We interpret this as partial disordering of boron atoms that were originally in a periodic array on the surface. Auger electron spectroscopy for films grown at 300 °C reveal a broadening of the ideal boron monolayer distribution by ≈ 5 Å due to surface segregation. This is consistent with the observation that $\approx 50\%$ of the boron remains in the ordered layer. Cross-sectional transmission electron microscopy and ion channeling studies show that the 100-Å-thick films grown at 300 °C are high quality crystalline silicon indistinguishable from bulk silicon, while room-temperature growth results in an amorphous layer.⁷

VII. ELECTRICAL PROPERTIES

We now discuss the electrical activity of boron doped silicon structures prepared via silicon surface reconstructions. Table I gives carrier densities and mobilities from low-tem-

TABLE I. Carrier densities and mobilities from low-temperature Hall effect measurements.

Surface orientation	Reconstruction	Overlayer	Boron coverage (ML)	Carrier density (ML)	Mobility ($\text{cm}^2 \text{V}^{-1} \text{s}^{-1}$)
100	2×1	Cryst.	0.44	0.45	21
100	2×1	Amorph.	0.50	0.24	1
111	$\sqrt{3} \times \sqrt{3}$	Amorph.	0.34	0.22	30
111	7×7	Amorph.	0.01	0	...

perature ($T = 4.2 \text{ K}$) Hall effect measurements for silicon overlayers grown at 30 and 300 °C. There was no carrier freeze-out and no significant magnetoresistance for any of the samples measured. Units of monolayers are used for clarity, where one monolayer is defined as $6.8 \times 10^{14} \text{ cm}^{-2}$ for Si(100) and $7.8 \times 10^{14} \text{ cm}^{-2}$ for Si(111). The optimum conditions for producing electrically active ordered doping layers in epitaxial silicon (100) are a boron coverage of 1/2 monolayer and a silicon growth temperature of 300 °C. Under these conditions 100% electrical activity and a mobility of $21 \text{ cm}^2 \text{V}^{-1} \text{s}^{-1}$ are obtained. This mobility is comparable to that obtained for very high boron concentrations in bulk silicon.¹¹ Table I also shows data for other structures including the (2×1) reconstruction of Si(100) and $\sqrt{3} \times \sqrt{3}$ reconstruction of Si(111) capped with amorphous silicon, and a control experiment in which the (undoped) Si(111)- (7×7) reconstruction was capped with amorphous silicon. The ordered structures involving boron represent the highest electrically active concentrations of dopants reported for any semiconductor. The proper description of these semiconductor/dopant systems as new alloys presents an interesting theoretical challenge.

VIII. CONCLUSIONS

We have shown that two-dimensional ordered layers of boron can be preserved at the Si(111) and Si(100) surfaces. In the Si(100) case epitaxial Si can be grown atop the ordered structure due to the low temperature required for (100) epitaxy. All systems show a high *p*-type electrical activity, between 50% and 100% electrically active.

ACKNOWLEDGMENTS

We thank Elias Vlieg, Ian Robinson, George Gilmer, and Dave Eaglesham for helpful discussions and other valuable contributions to this work.

- ¹J. M. Gibson, H.-J. Gossmann, J. C. Bean, R. T. Tung, and L. C. Feldman, *Phys. Rev. Lett.* **56**, 355 (1986); H.-J. Gossmann, L. C. Feldman, and W. M. Gibson, *ibid.* **53**, 294 (1984), *Surf. Sci.* **155**, 413 (1985); H.-J. Gossmann and L. C. Feldman, *Phys. Rev. B* **32**, 6 (1985).
- ²K. Akimoto, J. Mizuki, I. Hirose, T. Tatsumi, H. Hirayama, N. Aizaki, and J. Matsui, *Extended Abstracts on the 19th Conference of Solid State Devices and Materials* (Business Center for Academic Societies, Tokyo, 1987), p. 463.
- ³R. L. Headrick, L. C. Feldman, and I. K. Robinson, *Appl. Phys. Lett.* **55**, 442 (1989).
- ⁴R. L. Headrick, I. K. Robinson, E. Vlieg, and L. C. Feldman, *Phys. Rev. Lett.* **63**, 1253 (1989).
- ⁵R. L. Headrick, A. F. J. Levi, H. Luftman, J. Kovalchick, and L. C. Feldman (to be published).
- ⁶T. Tatsumi, I. Hirose, T. Nino, H. Hirayama, and J. Mizuki, *Appl. Phys. Lett.* **57**, 73 (1990).
- ⁷R. L. Headrick, B. E. Weir, A. F. J. Levi, D. J. Eaglesham, and L. C. Feldman, *Appl. Phys. Lett.* **57**, 2779 (1990).
- ⁸B. E. Weir, B. S. Freer, R. L. Headrick, J. Bevk, D. J. Eaglesham, G. H. Gilmer, and L. C. Feldman, *Appl. Phys. Lett.* (to be published).
- ⁹P. Bedrossian, R. D. Meade, K. Mortensen, D. M. Chen, and J. A. Golovchenko, *Phys. Rev. Lett.* **63**, 1257 (1989); I.-W. Lyo, E. Kaxiras, and Ph. Avouris, *ibid.* **63**, 1261 (1989).
- ¹⁰R. L. Headrick, B. E. Weir, D. J. Eaglesham, and L. C. Feldman, *Phys. Rev. Lett.* **65**, 1128 (1990).
- ¹¹D. J. Eaglesham, H.-J. Gossmann, and M. Cerullo, *Phys. Rev. Lett.* **65**, 1227 (1990).
- ¹²G. Masetti, M. Severi, and S. Solmi, *IEEE Trans. Electron. Dev.* **30**, 764 (1983).